

## **Clinical detection of cerebral microbleeds with quantitative susceptibility mapping in essential hypertension.**

**Qiong Wu, Guang Yao Wu\***

Department of Radiology, Zhongnan Hospital of Wuhan University, Donghu Road 165, Wuhan, PR China

### **Abstract**

**Objective:** To evaluate the magnetic susceptibility of Cerebral Microbleeds (CMBs) in patients with Essential Hypertension (EH) by Quantitative Susceptibility Mapping (QSM) sequence and to explore the application value of QSM sequence in CMBs of EH patients.

**Materials and methods:** A total of 33 EH patients with CMBs were enrolled in this study. The routine scan and QSM sequence were performed using the 3.0T Discovery750 Superconducting Magnetic Resonance Scanner. The distribution of CMBs in the spatial space was analyzed statistically. The relationship between the magnetic susceptibility of CMBs and the baseline data of EH patients was analyzed.

**Results:** 178 CMBs were observed with QSM sequence, which was significantly more than those of the conventional sequences. The number of CMBs was the largest in the basal ganglia-thalamus region, followed by the cortical-subcortical region. The magnetic susceptibility of CMBs was in the range of 0.112-0.494 and the mean value was 0.267, which was statistically different between the risk stratification groups. The susceptibility of basal ganglia-thalamus lesion was associated with risk stratification, systolic blood pressure, diastolic blood pressure, age and course of disease in EH patients. There was a positive correlation between the area of the QSM original image and the magnetic susceptibility value of the lesion in each region.

**Conclusion:** The QSM sequence can measure CMBs better than the conventional sequences. The CMBs of EH patients have the best incidence in the basal ganglia and the thalamus region, followed by the cortical-cortical area. The QSM sequence can provide favourable information for scientific studies and clinical applications in EH patients. And it can provide more imaging basis to understand the impact of hypertension on cerebral blood vessels and the occurrence of CMBs lesions, development, etc.

**Keywords:** Magnetic resonance imaging (MRI), Quantitative susceptibility mapping (QSM), Essential hypertension (EH), Cerebral microbleeds (CMBs).

*Accepted on August 28, 2017*

### **Introduction**

Cerebral Microbleeds (CMBs) are small chronic brain hemorrhages occurring in space around the small vessels of the brain, and may be caused by structural abnormalities of the small vessels [1]. With the progress of histopathology in CMBs, it has been found that CMBs are the aggregation of blood degradation products in the perivascular space. It is also believed that local magnetic field changes, which results from the transformation of blood exuded in the perivascular space to hemosiderin deposition, form the basis of imaging, and that hemolysin can be retained for a long time in macrophages locally exuded from the lesions [2,3]. Due to the local magnetic field changes caused by paramagnetic degradation products in the blood within the lesions, CMBs appear as small, quasi-circular low-signal-intensity areas, without surrounding edema, on MRI gradient echo sequence. Extensive studies demonstrate that the presence of CMBs are evidence of pathological changes in the vessel wall and that iron deposition

levels may suggest the nature and severity of vascular lesions [2,4-6]. Quantitative Susceptibility Imaging (QSM) provides a simple method for the quantitative analysis of iron deposition in CMBs. Therefore, this study provides a reference for understanding the relationship between CMBs and hypertension by determining the quantitative and spatial distribution of CMBs in hypertensive patients, as well as through quantitative analysis of iron deposition [3].

This study attempts to measure the number of CMBs in patients with Essential Hypertension (EH) by QSM and quantitatively analyze the iron deposition in the lesions. On this basis, it seeks to determine the pattern of magnetic susceptibility values and common sites of CMBs in EH patients, to compare the magnetic susceptibility of CMBs among the regions and between hypertension risk stratification groups, and to investigate the correlation between the baseline data. Finally, the correlation between the area of CMBs and its susceptibility value in each region is analyzed.

## Materials and Methods

### Subjects

Thirty-three patients with essential hypertension and CMBs, who were treated in the Department of Cardiology and Neurology of our hospital from November 2015 to January 2017, were enrolled. There were 19 males and 14 females, with an average age of  $66.4 \pm 6.3$  y. All patients met diagnostic criteria specified in 2010 Guidelines for prevention and treatment of hypertension in China. After consent was obtained from the patient and their family, and MRI contraindications were ruled out, conventional brain MRI, including axial T2 Weighted Imaging (T2WI), T1 Weighted Imaging (T1WI), Diffusion Weighted Imaging (DWI), sagittal T1WI and Enhanced Susceptibility-Weighted Angiography (ESWAN), was performed and followed by QSM. In addition, the patients were divided into low/moderate-risk and high/very high-risk groups according to the classification criteria specified in 2013 ESH/ESC Hypertension Guidelines. Subjects with secondary hypertension, central nervous system infectious diseases, brain tumors, Alzheimer's disease, Parkinson's disease, brain trauma, epilepsy, a history of central nervous system surgery, and severe organ failure were excluded.

### MRI protocol

**Conventional MRI:** A 3.0T Discovery 750 superconducting magnetic resonance scanner (GE Healthcare, USA), equipped with 8-channel NV coil, was used. 1WI parameters: TR/TE: 2133.2/24.0, FOV:  $240 \times 240$  mm, matrix:  $320 \times 256$ , slice thickness: 5.0 mm, slice gap: 1.5 mm, number of excitations: 1, bandwidth: 41.67. 2WI parameters: TR/TE: 9638.0/93.0, FOV:  $240 \times 240$  mm, matrix:  $320 \times 256$ , slice thickness: 5.0 mm, slice gap: 1.5 mm, number of excitations: 1, bandwidth: 83.333. ESWAN parameters: TR/TE=88 ms/8 ms, FOV: 24 cm, matrix:  $256 \times 256$ , slice thickness: 3 mm.

**QSM parameters:** TR/TE: 54.4/3.0, flip angle: 12 degrees, slice thickness/gap: 1.0/0.0 mm, matrix:  $220 \times 220$ , bandwidth: 62.50, number of echoes: 16, phase-encoded FOV: 1, acquisition time: 9 min 49 s.

### Imaging diagnosis

CMBs appeared as circular high-signal-intensity areas with a diameter of  $\leq 10.0$  mm on QSM. As the QSM sequence has not been widely used in clinical practice, the ESWAN sequence, which has long been applied, was still used for qualitative diagnosis of CMBs in this study. The observed lesions were analyzed by 2 deputy chief physicians. Cavernous hemangioma, venule and perivascular space were excluded based on plain scan images. According to the CMB grouping criteria (Charlotte et al.), the number of lesions was determined and the lesions were divided into cortical-subcortical, basal ganglia-thalamus and infratentorial regions. In event of disagreement, consensus was reached after discussion. Regions of interest were drawn for CMBs in each region to measure the lesion area. Magnetic susceptibility of the lesions was

measured three times on the QSM magnetic susceptibility map, and average values were calculated. Care was taken to avoid metal artifacts and partial volume effect of cerebrospinal fluid when measuring magnetic susceptibility. The GADW 4.6 FuncTool software (GE Healthcare, USA) was used. At the QSM post-processing interface, 0.04 was selected for Threshold (0-1) option and 14 15 16 for Echonumber by clicking the QSM key. Next, calculation was performed by clicking the Compute key to obtain Susceptibility and Phase images. Magnetic susceptibility values were recorded on the susceptibility images.

### Statistical analysis

Data were analyzed using SPSS 21 software. The rank sum test was used to compare the magnetic susceptibility of CMBs among the regions and between hypertension risk stratification groups. The Kruskal-Wallis test was used for pairwise comparison of the three groups of data. Spearman's rank correlation coefficient was used for correlations between the magnetic susceptibility of CMBs and blood pressure, gender, age and disease duration in EH patients, and between the area of CMBs on the original QSM images and the magnetic susceptibility. Enumeration data were analyzed by chi-square test.  $P < 0.05$  was considered statistically significant.

## Results

### 1. Detection of CMBs with QSM and conventional MRI:

For the 33 patients with EH, a total of 178 CMBs were detected with QSM, while 25 CMBs were detected with conventional MRI in 9 of the patients. The QSM was significantly superior to conventional MRI in CMB detection (Figure 1).

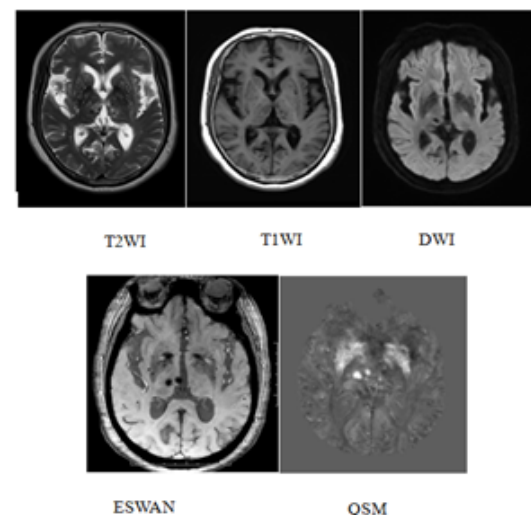


**Figure 1.** CMBs in the right thalamus revealed by conventional MRI, ESWAN, and QSM. CMBs appeared on ESWAN as circular or quasi-circular low-signal-intensity or signal loss areas with diameters less than 10 mm, without surrounding edema. They were visualized as high-signal-intensity areas on QSM.

**2. Differences in magnetic susceptibility of CMBs between the brain regions of EH patients:** In this study, 33 EH patients with CMBs were analyzed retrospectively. The brain was divided into cortical-subcortical, basal ganglia-thalamus, and infratentorial regions.

The magnetic susceptibility values of CMBs were measured to be 0.112 to 0.494. The rank sum test indicated significant differences in the magnetic susceptibility of CMBs among the three regions (P=0.000).

Pairwise comparison using the Kruskal-Wallis test revealed a significant difference in the magnetic susceptibility of CMBs between the basal ganglia-thalamus and cortical-subcortical regions (P=0.000) and between the basal ganglia-thalamus and infratentorial regions (P=0.008) but not between the cortical-subcortical and infratentorial regions (Table 1).

**Table 1.** Difference in CMB magnetic susceptibility among regions.

Region	n	M ± Q	P25	P75	Z	P
Cortical-subcortical	40	0.210 ± 0.084#	0.163	0.247	35.598	0
Basal ganglia-thalamus	117	0.282 ± 0.088# <sup>a</sup>	0.232	0.32		
Infratentorial	21	0.247 ± 0.131 <sup>a</sup>	0.169	0.3		
Total	178	0.260 ± 0.110	0.19	0.3		

Note: n is the number of CMBs, M is the median, Q is the interquartile range; P<0.05 represents a statistically significant difference; #Denotes a significant difference between the basal ganglia-thalamus and cortical-subcortical regions; <sup>a</sup>Denotes a significant difference between the basal ganglia-thalamus and infratentorial regions.

**3. Correlation between CMB area on the original QSM images and magnetic susceptibility in each region of EH patients:** The maximum area of CMBs was measured on the original QSM images, and the magnetic susceptibility of the corresponding CMBs was measured on the susceptibility maps. The Spearman test was used to analyze the correlation between the magnetic susceptibility of CMBs and their area in the cortical-subcortical, basal ganglia-thalamus, and infratentorial regions. The magnetic susceptibility was found to increase with the area in all the three regions (r=0.671, P=0.021 for cortical-subcortical region; r=0.734, P=0.000 for basal ganglia-thalamus region; r=0.752, P=0.031 for infratentorial region). It can be seen that the magnetic susceptibility values of CMBs increased with the lesion diameter in all regions. The results are shown in Table 2.

**Table 2.** Correlation between the area of the CMBs on the QSM original image and the magnetic susceptibility.

CMB a	Cortical-subcortical magnetic susceptibility		Basal ganglia-thalamus magnetic susceptibility		Infratentorial magnetic susceptibility	
	r	P	r	P	r	P
Area	0.671	0.021	0.734	0	0.752	0.031

Note: P<0.05 represents a statistically significant difference.

## Discussion

**1. Clinical significance of CMB magnetic susceptibility measurement with QSM:** Recently, with continuous improvement of calculation method, QSM has been more and more widely applied in the measurement of iron content in the brain [4]. However, QSM has been infrequently used to measure iron content in CMBs. That is what this study attempts to do. Patients with hypertension have higher iron content in the brain than normal people. Magnetic susceptibility is a characteristic of tissues. QSM provides quantitative information about the distribution of magnetic susceptibility in various brain regions [5]. Iron content in tissues has the greatest effect on the magnetic susceptibility value of the tissues. The magnetic susceptibility information obtained by QSM can accurately reflect the total iron concentration in tissues and provide important specific information for disease development and progression. A study compared the QSM findings with the actual iron concentrations determined by autopsy and found that the magnetic susceptibility values determined by QSM had a high specificity for the total iron concentrations in tissues, especially for Fe<sup>3+</sup> [6]. Iron ions are present in the form of Fe<sup>3+</sup> in hemosiderin within CMBs. This is the theoretical basis for detecting magnetic susceptibility of CMBs with QSM. There is a constant iron content in normal tissues [7]. The body has a poor ability to remove the abnormal deposition of iron ions. Abnormal iron content will cause histopathological changes of the tissue. The free radicals produced under the influence of iron ions can lead to destruction of the blood-brain barrier and thereby cause gradual neuronal apoptosis. In patients with Intracranial Hemorrhage (ICH), iron ions are significantly increased in the brain tissue and cerebrospinal fluid, and the expression of ferritin is also increased [8]. Iron ions in CMBs may play a vital role in pathological changes of the cerebrovascular wall. Therefore, the iron content in CMBs should be quantitatively analyzed, and iron load quantified [9].

**2. CMB distribution characteristics in EH patients:** In this study, CMBs were found to be mostly distributed in the basal ganglia-thalamus region of EH patients, followed by the cortical-subcortical region, and lastly the infratentorial region. This is consistent with previous studies. It indicates that the concentrated distribution of CMBs in deep brain of EH patients may be due to the fact that vascular pathological changes involved in hypertension mainly occur in deep perforating arteries [10].

Some scholar reported that hypertensive intracerebral hemorrhage typically occurred in thalamus, putamen, pons, and cerebellum [11]. The lack of collagen IV results in fragmentation of the vascular wall. As the most common type of vascular wall injury, hypertension-induced hyaline degeneration can lead to loosening of the cerebrovascular wall, which in turn results in CMBs. Extensive deposition of β-amyloid in the small vessel wall has been considered to be another important reason for increased vascular fragility [12].

Both types of vascular disease significantly affect the strength of the vessel wall. Histological changes, such as local aggregation of macrophages and leukocytes, and lacunar state in basal ganglia, are often observed for collagen abnormalities around CMBs in patients with ICH. Moreover, such changes indicate a high risk of cerebral hemorrhage [13]. In addition, the common sites of CMBs observed in this study are the same as those of ICH. The occurrence of ICH may be closely related to CMBs. Many studies also suggest that the presence of CMBs is an independent risk factor for spontaneous intracerebral hemorrhage. CMBs in the cortical-subcortical region are associated with smoking, APOE $\epsilon$ 4, and low cholesterol levels [14]. Cerebral amyloid angiopathy also commonly occurs in the cortical-subcortical region.

### 3. Magnetic susceptibility values of CMBs in each region:

The magnetic susceptibility value of CMBs in the basal ganglia-thalamus region were shown to be significantly different from those in the basal ganglia-thalamus and infratentorial regions. The possible reason is the different degree of pathological changes of involved vessels among each region. Cerebral vessels involved in hypertension are mainly in the basal ganglia, thalamus, pons, brain stem, and cerebellar hemisphere. The pathological changes of the blood vessel wall in the basal ganglia-thalamus region were more severe than those in other regions, which led to more exudation of blood components in this region, thus resulting in increased iron deposition in CMBs. Therefore, the determination of magnetic susceptibility in CMBs can provide some reference for the pathogenesis and development of cerebrovascular pathological changes caused by hypertension.

**4. Relationship between the CMB area on original QSM images and the magnetic susceptibility value:** Owing to the blooming effect, the lesion area on the magnetic susceptibility map is larger than the actual area, which may lead to inaccurate results. The measurement of CMB area using the original QSM images can accurately reflect the actual area. CMBs appeared as low-signal-intensity areas with a clear boundary. The measurement was based on the maximum area on the original axial images. The magnetic susceptibility values of CMBs in EH patients were found to be increased with the area in all the three regions. It suggests that the iron content in CMBs of EH patients increases with the area. This finding demonstrates that the total iron content in CMBs of EH patients is positively correlated with the area. It may mean that the increased iron content promotes the vascular wall injury in the region, which increases the CMB diameter in the basal ganglia-thalamus region and thus further affects the occurrence of ICH [15,16].

## Conclusion

QSM can well reflect tissue susceptibility. The magnetic susceptibility of CMBs in EH patients follow a certain spatial pattern: It is higher in the basal ganglia region than in the basal ganglia-thalamus and infratentorial regions. This can better detect and diagnose CMBs and provide quantitative analysis of CMBs, in order to provide more useful information for clinical practice.

## Acknowledgments

This study has received funding by Major Program of the National Natural Science Foundation of China (Grant No. 81227902) and national key basic research program National Natural Science Foundation of China (Grant No. 2016YFC1304702).

## Declaration of Conflict of Interests

No conflicts of interest. We are responsible for the content and writing of the paper.

## References

1. Paul A, Victor LV. Cerebral microbleeds: a review of clinical, genetic and neuroimaging associations. *Front Neurol* 2014; 4: 205.
2. Scharf J, Brauherr E, Forsting M, Sartor K. Significance of haemorrhagic lacunes on MRI in patients with hypertensive cerebrovascular disease and intracerebral haemorrhage. *Neuroradiol* 1994, 36: 504-508.
3. Jeon SB, Kang DW, Cho AH, Lee EM, Choi CG, Kwon SU. Initial microbleeds at MR imaging can predict recurrent intracerebral hemorrhage. *J Neurol* 254: 508-512.
4. Meike WV. Cerebral microbleeds: do they really predict macrobleeding? *Int J Stroke* 2012; 7: 565-566.
5. Charidimou A, Werring DJ. Cerebral microbleeds: detection, mechanisms and clinical challenges. *Futur Neurol* 2011; 6: 587-611.
6. Charidimou A, Werring DJ. Letter by Charidimou and Werring regarding article, "Cerebral microbleeds in the elderly". *Stroke* 2011; 42: e368.
7. Lee SH, Bae HJ, Kwon SJ. Cerebral microbleeds are regionally associated with intracerebral hemorrhage. *Neurol* 2004; 62: 72-76.
8. Reichenbach JR, Schweser F, Serres B, Deistung A. Quantitative susceptibility mapping: Concepts and applications. *Clin Neuroradiol* 2015; 25: 225-230.
9. Jeam HOB, Rafael E. Correlation between paramagnetic ions and quantitative susceptibility values of post-mortem brain study. *ISMRM* 2015.
10. Poels MM, Vernooij MW, Ikram MA, Hofman A, Krestin GP, van der Lugt A, Breteler MM. Prevalence and risk factors of cerebral microbleeds: an update of the Rotterdam Scan Study. *Stroke* 2010; 41: 103-106.
11. Martinez-Ramirez S, Greenberg SM, Viswanathan A. Cerebral microbleeds: overview and implications in cognitive impairment. *Alzheimers Res Ther* 2014; 6: 1-7.
12. Wu Y, Chen T. An up-to-date review on cerebral microbleeds. *J Stroke Cerebrovasc Dis* 2016; 25: 1301-1306.
13. Forouzanfar MH, Alexander L. Global, regional, and national comparative risk assessment of 79 behavioural, environmental and occupational, and metabolic risk factors or clusters of risks in 188 countries, 1990-2013: a

- systematic analysis for the Global Burden of Disease Study 2013. *Lancet* 2015; 386: 2287-2323.
14. Kearney PM, Whelton M, Reynolds K, Muntner P, Whelton PK, He J. Global burden of hypertension: analysis of worldwide data. *Lancet* 2005; 365: 217-223.
15. Scharf J, Brauherr E, Forsting M. Significance of haemorrhagic lacunes on MRI in patients with hypertensive cerebrovascular disease and intracerebral haemorrhage. *Neuroradiol* 1994; 36: 504-508.
16. Cordonnier C, Potter GM, Jackson CA, Doubal F, Keir S, Sudlow CL, Wardlaw JM, AlShahi Salman R: Improving interrater agreement about brain microbleeds: development of the Brain Observer MicroBleed Scale (BOMBS). *Stroke* 2009; 40: 94-99.

**\*Correspondence to**

Guang Yao Wu

Department of Radiology

Zhongnan Hospital of Wuhan University

PR China